

## Detecting and predicting land use and land cover changes in eastern Nile-delta of Egypt using CA-Markov

Waleed Maged<sup>[1][2]</sup>, Caiyun Wang<sup>\*[1]</sup>

College of Electronic and Information Engineering

<sup>1</sup>Nanjing University of Aeronautics and Astronautics, Nanjing 210016, China

<sup>2</sup>National Gene Bank (NGB), Agricultural Research Centre (ARC), Egypt

\*College of Astronautics

<sup>1</sup>Nanjing University of Aeronautics and Astronautics, Nanjing 210016, China

Email: wangcai Yun@nuaa.edu.cn

### Abstract

Information about changes in land use/land cover (LULC) is very useful for local governments and urban planners in setting future plans for the sustainable development. The main objectives of this work were to study changes in LULC in two governorates located at the eastern region of Nile-delta in Egypt and to expecting their future changes using CA-Markov model. Accordingly, Landsat images were images collected at three time periods (1999, 2009 and 2019). These images were manipulated and analyzed for LULC and their changes in studied area. CA-Markov integrated approach was used to predict future changes in LULC within this area. In this context, Geographic information systems (GIS) and remote sensing methodology provide essential tools which can be applied in the analysis of land use change detection.

**Keywords:** LULC, ERDAS, GIS, IDRISI, CA-Markov, Remote Sensing, Egypt.

### 1. INTRODUCTION

Land use and land cover change, as one of the key driving forces of global environmental change, Land use/land cover change has been reviewed from different perspectives in order to identify the drivers of land use/land cover change, their process and consequences. The rapid changes in land use and cover than ever before, especially in developing nations, are often characterized by widespread urban spreading, land destruction, or the transformation in agricultural land to shrimp farming resulting enormous cost to the environment [1]. This kind of changes deeply affects local and/or national climate, which will inevitably impact the global environment. Human induced changes in land cover for instance,

affect the global carbon cycle, and lead to the rise in atmospheric carbon oxide [2]. It is therefore imperative to investigate the changes in land use/cover, so that its impact on terrestrial environment can be discerned, and sustainable land use planning can be formulated [3].

In Egypt, only approximately 4% of Egypt's total area is agricultural land, and this area has one of the highest population densities in the world. The remaining 96% of the land is arid desert. Seen from this perspective, the need for reclamation of the desert appears inevitable in light of continued population growth and increased congestion in the long-settled lands in the Nile valley and the delta [4]. Remote sensing and its applications emerged in Egypt as early as the invention of this technology [5].

For this purpose, the temporal dynamics of remote sensing data can play an important role in monitoring and analyzing land cover changes. Accurate and up-to-date land cover change information is necessary to understanding and assessing the environmental consequences of such changes [6]. While remote sensing has the capability of capturing such changes, extracting the change information from satellite data requires effective and automated change detection techniques [7].

Digital change detection is the process of determining and/or describing changes in land cover and land-use properties based on co-registered multi-temporal remote sensing data. The basic premise in using remote sensing data for change detection is that the process can identify change between two or more dates that is uncharacteristic of normal variation.

Numerous researchers have addressed the problem of accurately monitoring land-cover and land-use change in a wide variety of environments [8].

As such, Cellular Automata (CA)-Markov is a series of random values whose likelihood of occurrence in a given time interval is dependent on the values of the past. As a stochastic model, the CA-Markov model is able to analyses the land cover and use images related to two time periods, so as to generate the transition probability matrix [9, 10].

The Markov chain model component controls time dynamics between land-use categories via transition probabilities, while spatial dynamics are automatically guided by local rules defined by Cellular Automata (CA)-Markov spatial filters or potential transition maps, the matrix of transition probability generated by the Markov chain model is one of the entries in CA Model [11]. Therefore, the CA-Markov model successfully integrates the benefits of the Markov and CA models. The accuracy of spatial prediction can be modeled efficiently at the same time, and the prediction steps with the CA-Markov model involve 1) the construction of the MCE-based suitability atlas; 2) the generation of the transfer matrix and the state of transition probability matrix by means of the Markov model; 3) the prediction of future land use using the CA model [12].

The aims of the this study are to produce a land use/land cover map and Future prediction of Area Study by using GIS and Remote Sensing.

## 2. MATERIALS AND METHODS

### 2.1. DESCRIPTION OF STUDY AREA

Cover the area study two governorates from Egypt, which Ismailia and Sharkia. It is located between these coordinates 31° 15' 25.068" E to 32° 48' 30.238" E and 30° 9' 44.788" N and 31° 6' 31.831" N. It is bordered by North Sinai governorate from the East, Gharbia governorates from the West, Suez and Qalyubia governorates from the South and Port Said and Manzala Lake from the North (Fig.1).

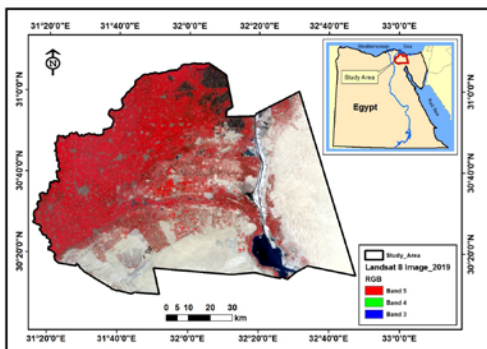


Fig 1. Location map of the studied area.

### 2.2. LANDSAT DATA

Landsat images were used in this study to evaluate land use/cover changes over three periods of time (1999, 2009 and 2019). The studied area is located in only one Landsat image (path 176, row 39). Three images were used to study the spatial and temporal changes in agricultural lands at Ismailia and Sharkia governorates in Egypt, during 1999, 2009 and 2019. Landsat data were downloaded for free from the earth explorer website established by the United States Geological Survey, <http://earthexplorer.usgs.gov/>. The studied images were acquired during the winter season. The acquisition dates and type of sensor are represented in table 1.

Table 1 Type of sensor, acquisition date, path, row and source of the studied Landsat images.

Type of sensor	Acquisition date	Path/Row	Source
Landsat 8 (OLI)	13/03/2019	176/39	USGS
Landsat 5 (TM)	13/02/2009	176/39	USGS
Landsat 5 (TM)	06/03/1999	176/39	USGS

### 2.3. ATMOSPHERIC AND GEOMETRIC CORRECTIONS

Atmospheric and radiometric corrections were carried out on the three studied Landsat images to minimize the atmospheric interferences by using ERDAS software package (ver. 2015). All images were projected to have the same projection (UTM, Zone 36N, Datum WGS 1984). A false color composite of the studied images is illustrated in figures 2, 3 and 4.

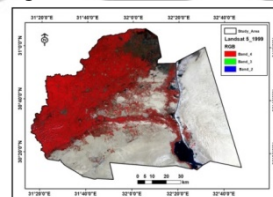


Fig. (2). False color composite of the studied Landsat 5 image in 1999.

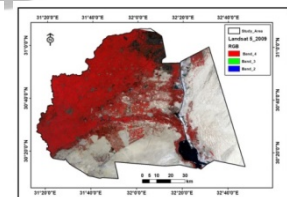


Fig. (3). False color composite of the studied Landsat 5 image in 2009.

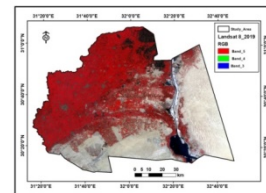


Fig. (4). False color composite of the studied Landsat 8 image in 2019.

### 2.4. MAXIMUM LIKELIHOOD SUPERVISED CLASSIFICATION

Maximum likelihood supervised classification is the most commonly used land use/cover classification algorithm worldwide. It is based on the assumption that the training data statistics in each spectral band are normally distributed. It considers that the distances towards class means and it calculates the variance-covariance matrix for each

class. In this method the supervised classification begins with defining the areas that will be used as training sites for the different land cover classes [13]. They also require a large training data set which can be very costly and generally not possible to add incrementally to the training data while training the classifier. A minimum of 15 samples was selected for each class. Ideally, the number of pixels selected should be more than 10 times as many pixels as there are bands in the image to be classified [14]. This was made with several training sites for the more training site selected, the better the results gained. Table 2 shows a description of LULC classification scheme.

Table 2. Land Use/Land Cover Classification Scheme.

Class	Description
Crop Land	Areas cultivated with annual crops, vegetables, or fruit. These crops are mainly irrigated by water from the river Nile and/or ground water. Most of the cultivated areas are newly reclaimed.
Urban Area	Includes construction activities along the coastal dunes (summer resorts) as well as sporadic houses of the Bedouins within the local villages and some governmental buildings.
Water	Includes all water bodies in the studied area
Sand Dunes	Include hills of loose sand built by aeolian processes or the flow of water
Sabkha	Sabkha is an Arabic name for a salt-flat ordinarily found nearby sand dunes. The low-lying sabkha is a landscape of sand cemented into a fragile crust by the alkaline minerals of a high water table.
Bare Land	Land areas of exposed soil surface as influenced by human impacts and/or natural causes.
Fish Farms	Water pools that are used for growing fish.

### 2.5. ACCURACY ASSESSMENT

Accuracy Assessment was carried out on the LULC classification images in 1999, 2009 and 2019. This was to evaluate the accuracy of each of the assigned LULC class. The classified image was matched with a variety of data such as aerial photographs and high resolution satellite image for the 2019 images. Four types of accuracy were calculated for each classified image, which are: 1. producer's accuracy; 2. user's accuracy, 3. overall accuracy; and Kappa coefficient as described by Campbell and Wynne [15].

### 2.6. CHANGE DETECTION ANALYSIS

Change detection analyses identify and measure variations between images of the same scene at different times. The classified images of the three studied dates were used to quantify and calculate the area of each LULC and detect changes that happened in it. This analysis is very helpful in recognizing various changes that took place in the different classes of LULC including the increase and/ or decrease in agricultural land and urban areas.

### 2.7. LULC CHANGE PREDICTION

CA-Markov is a strong approach for predicting changes in LULC. It is recommended because it out performs compared to other methods [16, 17, 18]. It can also predict two-way transitions between LULC classes [19]. Simulation and future land use change prediction were conducted in IDRISI-Selva software environment. Predictions of future LULC change using a CA-Markov model occurred in three steps: 1) applying the Markov chain analysis to the 1999, 2009, and 2019 LULC maps for calculating transition matrices; 2) calculating transition potential maps of LULC; and 3) application of the CA model to the transition matrices and the transition potential maps to predict the spatial distribution of LULC.

## 3. RESULTS AND DISCUSSIONS

### 3.1. Changes in land use/land cover classification within the studied area

Maximum likelihood supervised classification was carried out to evaluate land use/cover in the studied area in 1999, 2009 and 2019. It was executed using the ArcGIS 10.4 software package. There were seven land use / cover in the studied area. They are crop lands, urban areas, water, sand dunes, Sabkha, bare land and fish farms.

The study area has witnessed increased crop land and urban land change in different LULC. The results of the accuracy assessment of the classified imageries of the year's 1999, 2009, and 2019 indicates that the land use changes have been accurately identified and extracted during the classification, which is also confirmed by the overall accuracies and Kappa accuracy (Table 3).

Table 3 Accuracy assessments of classified LULC maps for the years 1999, 2009, and 2019.

LULC classes	1999		2009		2019	
	Producer's Accuracy %	User's Accuracy %	Producer's Accuracy %	User's Accuracy %	Producer's Accuracy %	User's Accuracy %
Crop Land	94.69	87.11	94.63	86.61	96.15	87.72
Urban Area	72.22	79.59	71.70	76.00	75.00	85.71
Water	78.95	88.24	77.78	82.35	100.00	88.89
Sand Dunes	89.55	98.36	89.39	96.72	89.86	98.41
Sabkha	78.26	78.26	77.27	73.91	90.00	78.26
Bare Land	80.85	91.57	80.22	89.02	81.91	91.67
Fish Farms	72.22	61.90	72.22	60.47	72.97	77.14
Overall accuracy	86.00		84.20		88.40	
Kappa accuracy	0.81		0.82		0.84	

The areas and percentages of the studied LULC classes are represented in Table 4. Also, the spatial distribution of these classes within the studied area is illustrated in figures 5, 6 and 7. Crop land areas were increased over the studied period of time from 4056.24 km<sup>2</sup> (39.79%) in 1999 to 4986.95 km<sup>2</sup>

(48.91%) in 2019. This increase in crop lands could be attributed to the increase in land reclamation and cultivation projects in this area. Urban areas were also increased from 1999 to 2019. These areas were about 375.14 km<sup>2</sup> (3.68%) in 1999 and 809.41 km<sup>2</sup> (7.94%) in 2019. This increase in urban areas could be due to the constant increase in population

On the other hand, sand dune areas were decrease from 1763.58 km<sup>2</sup> (17.30%) in 1999 to 1424.12 km<sup>2</sup> (13.97%) in 2019. This could be attributed to the stabilization of these sand dunes and using them in urban or agricultural activities. Bare lands were decreased from 2833.97 km<sup>2</sup> (27.80%) in 1999 to 2041.90 km<sup>2</sup> (20.03%) in 2019. This also could be attributed to the conversion of these areas into urban areas. Fish farms were also decreased from 725.83 km<sup>2</sup> (7.12%) in 1999 to 480.14 km<sup>2</sup> (4.71%) in 2019. Some of these areas were converted into crop lands.

There wasn't significant increase in both water and Sabkha areas during this period of time. Water areas were about 201.85 km<sup>2</sup> (1.98%) in 1999 and 193.68 km<sup>2</sup> (1.90%) in 2019. Sabkha areas were about 237.53 km<sup>2</sup> (2.33%) in 1999 and 258.94 km<sup>2</sup> (2.54%) in 2019

Table 4: Areas and percentages of land use/land cover within the studied area in 1999, 2009 and 2019.

LULC Type	1999		2009		2019	
	Area (km <sup>2</sup> )	%	Area (km <sup>2</sup> )	%	Area (km <sup>2</sup> )	%
Crop Land	4056.24	39.79	4404.89	43.21	4985.95	48.91
Urban Area	375.14	3.68	726.87	7.13	809.41	7.94
Water	201.85	1.98	197.76	1.94	193.68	1.90
Sand Dunes	1763.58	17.30	1600.47	15.70	1424.12	13.97
Sabkha	237.53	2.33	405.72	3.98	258.94	2.54
Bare Land	2833.97	27.80	2269.21	22.26	2041.90	20.03
Fish Farms	725.83	7.12	589.22	5.78	480.14	4.71
	10194.14	100.00	10194.14	100.00	10194.14	100.00

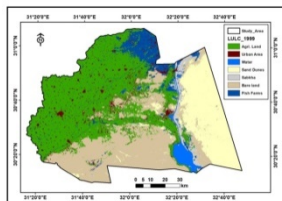


Fig 5. Spatial distribution of Land use/land cover classes within the studied area in 1999

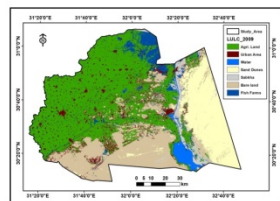


Fig 6. Spatial distribution of Land use/land cover classes within the studied area in 2009

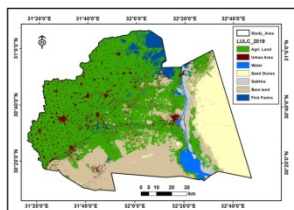


Fig 7. Spatial distribution of Land use/land cover classes within the studied area in 2019

### 3.2. Markov chain matrix of LULC

#### 3.2.1. Transition probabilities matrix from 1999 to 2009

The transition probability matrix for the period from 1999 to 2009 was calculated using CA-Markov as shown in Table 5. This transition probability matrix gives the future probability percentage of land use change during this period of time. It shows that about 12% of crop lands are expected to change into urban areas. At the same time, about 29% of urban areas are expected to be converted in to crop lands. This table also shows that about 14.5 % of bare land is expected to be converted into crop land and 11.4% of it is expected to be transit into urban area. Also, about 36% of fish farms are expected to be converted into crop lands.

Table5. Markov chain matrix of LULC transition probabilities from 1999 to 2009

LULC Type	Crop Land	Urban Area	Water	Sand Dunes	Sabkha	Bare Land	Fish Farms
Crop Land	0.790	0.123	0.000	0.001	0.012	0.024	0.050
Urban Area	0.288	0.564	0.001	0.001	0.007	0.031	0.109
Water	0.002	0.005	0.813	0.000	0.034	0.005	0.142
Sand Dunes	0.026	0.019	0.000	0.736	0.046	0.171	0.004
Sabkha	0.099	0.042	0.003	0.024	0.590	0.140	0.102
Bare Land	0.145	0.114	0.000	0.034	0.075	0.611	0.021
Fish Farms	0.358	0.086	0.007	0.001	0.043	0.017	0.489

#### 3.2.2. Expected Transition matrix from 1999 to 2009

Table 6 shows the expected transition in areas for each land use/cover class from 1999 to 2009. It indicates that about 540.58 km<sup>2</sup> of crop lands are expected to be converted to urban area, whereas about 209.26 km<sup>2</sup> are expected to be converted from urban area to crop land. Also, about 328.81 km<sup>2</sup> of bare land and 210.77 km<sup>2</sup> of fish farms are expected to be changed into crop land. About 258.40 km<sup>2</sup> of bare land are expected to be converted into urban area.

Table 6 Expected transition in areas (km<sup>2</sup>) from 1999 to 2009

LULC Type	Crop Land	Urban Area	Water	Sand Dunes	Sabkha	Bare Land	Fish Farms
Crop Land	3476.3	540.58	0.02	3.83	54.38	107.22	220.25
Urban Area	209.26	409.56	0.61	0.61	5.16	22.25	78.62
Water	0.33	0.91	162.03	0.00	6.65	1.06	27.98
Sand Dunes	41.30	29.58	0.00	1179.0	73.22	273.55	5.57
Sabkha	40.38	16.96	1.15	9.94	239.57	56.78	41.30
Bare Land	328.81	258.40	0.23	76.16	170.16	1385.7	48.48
Fish Farms	210.77	50.45	4.26	0.57	25.52	9.84	287.15
Total	4307.2	1306.4	168.29	1270.1	574.66	1856.4	709.34

**3.2.3. Transition probabilities matrix from 2009 to 2019**

The transition probability matrix for the period from 2009 to 2019 was calculated using CA-Markov as shown in Table 7. This transition probability matrix gives the future probability percentage of land use change during this period of time. It shows that about 13% of crop lands are expected to change into urban areas. At the same time, about 42.5% of urban areas are expected to be converted in to crop lands. This table also shows that about 21.5 % of bare land is expected to be converted into crop land. Also, about 33% of fish farms are expected to be converted into crop lands.

**Table 7. Markov chain matrix of LULC transition probabilities from 2009 to 2019**

LULC Type	Crop Land	Urban Area	Water	Sand Dunes	Sabkha	Bare Land	Fish Farms
Crop Land	0.793	0.128	0.000	0.000	0.003	0.043	0.033
Urban Area	0.424	0.406	0.001	0.000	0.003	0.110	0.057
Water	0.009	0.000	0.786	0.000	0.045	0.005	0.155
Sand Dunes	0.028	0.002	0.001	0.720	0.024	0.223	0.002
Sabkha	0.326	0.019	0.012	0.016	0.338	0.231	0.059
Bare Land	0.214	0.023	0.000	0.044	0.033	0.680	0.006
Fish Farms	0.329	0.072	0.012	0.000	0.045	0.031	0.512

**3.2.4. Expected Transition matrix from 2009 to 2019**

Table 8 shows the expected transition in areas for each land use/cover class from 2009 to 2019. It indicates that about 620.04 km<sup>2</sup> of crop lands are expected to be converted to urban area, whereas about 255.91 km<sup>2</sup> are expected to be converted from urban area to crop land. Also, about 479.39 km<sup>2</sup> from bare land to crop land and 157.89 km<sup>2</sup> of fish farms are expected to be changed into crop land. About 49 km<sup>2</sup> of bare land are expected to be converted into urban area.

**Table 8 Expected transition in areas (km<sup>2</sup>) from 2009 to 2019**

LULC Type	Crop Land	Urban Area	Water	Sand Dunes	Sabkha	Bare Land	Fish Farms
Crop Land	3943.9	620.04	0.36	0.92	13.27	214.75	165.05
Urban Area	255.91	239.05	0.31	0.11	1.98	66.38	34.15
Water	1.72	0.01	153.71	0.00	8.68	0.96	30.12
Sand Dunes	40.12	2.71	0.80	1061.1	34.76	317.09	3.04
Sabkha	84.41	4.68	3.19	4.26	87.74	60.02	15.21
Bare Land	479.39	49.00	0.68	102.32	73.45	1524.0	13.56
Fish Farms	157.89	33.83	5.55	0.02	21.55	14.94	245.68
Total	4963.4	949.33	164.59	1168.8	241.43	2198.1	506.82

**3.3. Predicted LULC in 2019 and 2030**

The land use/ cover maps for 1999 and 2009 were used to predict the LULC map in 2019 using the CA-Markov model. The LULC map in 2019 was predicted at moderate accuracy (Kappa standard index= 0.80 and the kappa location index= 0.89). Similarly, the LULC maps for 2009 and 2019 were used to predict the expected changes in LULC class in 2030. Data in Table 9 show the area and its percentage for each land use/cover class in both 2019 and 2030 and the expected differences between them. These data indicate that the most significant increase is expected to be in urban areas, whereas the significant decrease is expected to be in sand dunes. There were no significant expected differences in the other land use/ cover classes in 2030. These results also indicate that the increase in crop land due to land reclamation projects doesn't cover the transition of current crop lands into urban areas. The predicted LULC map of the studied area in 2019 and 2030 is illustrated in Fig. 8 and 9.

**Table 9 Predicted LULC in 2019 and 2030**

LULC Type	2019		2030		Net difference	
	Area (km <sup>2</sup> )	%	Area (km <sup>2</sup> )	%	Area (km <sup>2</sup> )	%
Crop Land	4985.95	48.91	4964.99	48.70	-20.96	-0.21
Urban Area	809.41	7.94	949.33	9.31	139.92	1.37
Water	193.68	1.90	164.59	1.61	-29.09	-0.29
Sand Dunes	1424.12	13.97	1168.82	11.47	-255.3	-2.5
Sabkha	258.94	2.54	241.43	2.37	-17.51	-0.17
Bare Land	2041.90	20.03	2198.16	21.57	156.26	1.54
Fish Farms	480.14	4.71	506.82	4.97	26.68	0.26
Total	10194.14	100.00	10194.14	100.00	0	0

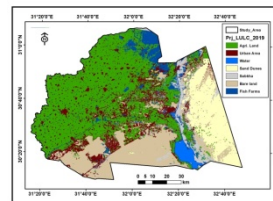


Fig. 8. Predicted land use/ cover in 2019 using CA-Markov model.

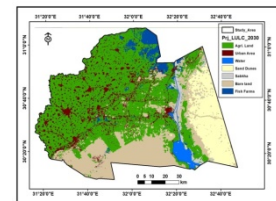


Fig. 9. Predicted land use/ cover in 2030 using CA-Markov model.

**4. CONCLUSION**

It could be concluded that CA-Markov model could help in predicting future expected changes in LULC. It was observed that the most significant changes in LULC within the studied area were in crop lands and urban areas. Urban areas were increased over time due to the consistent increase in population. Crop land areas were also increased over time; however this increase doesn't match their decrease due to urban encroachment. Accordingly, the final results show no evident increase in the total area of crop lands. Part of bare lands was converted

into both crop land and urban areas. Also, fish farms were changed into crop lands. Finally, these results help in directing future expansion and development in urban areas towards bare lands in the studied area. This is to sustain the existing crop lands to meet the needs of the increasing population for food, fiber and fuel.

#### ACKNOWLEDGEMENT

This work was supported in part by the National Natural Science Foundation of China under Grant No. 61301211 and China Scholarship Council No. 201906835017

#### REFERENCES

- [1] Sankhala, S., Singh, B., 2014. Evaluation of urban sprawl and land use land cover change using remote sensing and GIS techniques: a case study of Jaipur City, India. *Int. J. Emerging Technol. Adv. Eng.* 4 (1),66–72.
- [2] Alves, D., Skole, D., 1996. Characterizing land cover dynamics using multi-temporal imagery. *Int. J. Remote Sen.* 17 (4), 835–839.
- [3] Mutitanon, W., Tripathi, N., 2005. Land use/cover changes in the coastal zone of Bay Don Bay, Thailand using Landsat 5 TM data. *Int. J. Remote Sen.* 26 (11), 2311–2323.
- [4] Adriansen, H. K. (2009). Land reclamation in Egypt: a study of life in the new lands. *Geoforum*, 40(4), 664e674.
- [5] El-Baz, F., Breed, C., Grolier, J., McUauley, J., 1979. Eolian features in the western desert of Egypt and some applications to Mars. *J. Geophys. Res.* 84, 8205–8221.
- [6] Giri, C., Zhu, Z., & Reed, B. (2005). A comparative analysis of the Global Land Cover 2000 and MODIS land cover data sets. *Remote Sensing of Environment*, 94, 123–132.
- [7] Roy, D. P., Lewis, P. E., & Justice, C. O. (2002). Burned area mapping using multi-temporal moderate spatial resolution data—a bi-directional reflectance model-based expectation approach. *Remote Sensing of Environment*, 83, 263–286.
- [8] Chan, J. C., Chan, K. P., & Yeh, A. G. O. (2001). Detecting the nature of change in an urban environment: A comparison of machine learning algorithms. *Photogrammetric Engineering and Remote Sensing*, 67,213-225
- [9] Halmy MWA, Gessler PE, Hicke JA, Salem BB. Land use/land cover change detection and prediction in the north-western coastal desert of Egypt using CA-Markov. *Applied Geography*. 2015;63:101-12.
- [10] Kaveh N, Ebrahimi a. Prediction of land use / cover changes Using CA- Markov model. *Journal of applied remote sensing and gis in natural resource*. 2013;2.
- [11] Singh, S.K.; Laari, P.B.; Mustak, S., (2017). Modelling of land use land cover change using earth observation data-sets of Tons River Basin, Madhya Pradesh, India *Geocarto. Int.*, 1–21 (21 pages).
- [12] Liping, C.; Yujun, S.; Saeed, S., (2018). Monitoring and predicting land use and land cover changes using remote sensing and GIS techniques—A case study of a hilly area, Jiangle, China. *PLoS One*, 13: e0200493 (11 pages).
- [13] Currit, N. (2005) Development of a Remotely Sensed, Historical Land-Cover Change Database for Rural Chihuahua, Mexico. *International Journal of Applied Earth Observation and Geoinformation*, 7, 232-247. <http://dx.doi.org/10.1016/j.jag.2005.05.001>
- [14] Jensen, J.R. (2005) *Introductory Digital Image Processing: A Remote Sensing Perspective*. 3rd Edition, Pearson Prentice Hall, Upper Saddle River.
- [15] Campbell, J.B. and Wynne, R.H. (2011). *Introduction to remote sensing*, New York: Guilford, 5,P. 667.
- [16] Theobald, D. M., & Hobbs, N. T. (1998). Forecasting rural land-use change: a comparison of regression- and spatial transition-based models. *Geographical and Environmental Modelling*, 2, 65e82.
- [17] Parker, D. C., Manson, S. M., Janssen, M. A., Hoffmann, M. J., & Deadman, P. (2003). Multi-agent systems for the simulation of land-use and land-cover change: a review. *Annals of the Association of American Geographers*, 93, 314e337.
- [18] Kamusoko, C., Aniya, M., Adi, B., & Manjoro, M. (2009). Rural sustainability under threat in Zimbabwe e simulation of future land use/cover changes in the Bindura district based on the Markov-cellular automata model. *Applied Geography*, 29, 435e447.
- [19] Pontius, G. R., & Malanson, J. (2005). Comparison of the structure and accuracy of two land change models. *International Journal of Geographical Information Science*, 19, 243e265.